Available online at www.sciencedirect.com
SCIENCE DIRECT
ACADEMIC PRESS
Journal of Sound and Vibration 269 (2004) 781–793
JOURNAL OF SOUND AND VIBRATION
www.elsevier.com/locate/jsvi

Meshless formulation using NURBS basis functions for eigenfrequency changes of beam having multiple open-cracks

S.C. Fan*, N. Sheng

School of Civil and Environmental Engineering, Nanyang Technological University, Nanyang Avenue, Singapore 639798, Singapore

Received 7 January 2002; accepted 16 January 2003

Abstract

This paper presents a meshless formulation using non-uniform rational B-spline (NURBS) basis functions, and its applications to evaluate natural frequencies of a beam having multiple open-cracks. Node-based NURBS basis functions are used to construct the approximation function. The characteristic differentiability of the NURBS basis functions allows it to represent a function having specific degrees of smoothness and/or discontinuity. The discontinuity can be incorporated simply by assigning multiple knots at those locations. Hence, it can yield exact solutions having interior discontinuous derivatives. These advantages of NURBS are well known, and have been used extensively in graphical approximation of geometrical surfaces. However, it is seldom used in other engineering applications. To model the multiple open-cracks in a beam, quartic NURBS basis functions are employed and quadruplicate knots are assigned at the crack locations. Hence, it is capable to model the abrupt changes of slope (the first derivative of displacement) across a crack. In the present applications, additional equivalent massless rotational springs are inserted at the crack locations to represent the local flexibility caused by the cracks. As such, the cracked beam can be treated in the usual manner as a continuous beam. By adopting the meshless Petrov–Galerkin formulation, a generalized stiffness matrix for the cracked beam can be derived. Compared to the conventional finite element method, the present method does not require a finite element mesh for the purposes of interpolation and numerical integration. The advantages and effectiveness of the present method is illustrated in solving the eigenfrequencies of a beam having multiple open-cracks of different depths.

*Corresponding author. Fax: +65-679-106-76.
E-mail address: cfansc@ntu.edu.sg (S.C. Fan).

0022-460X/03/$ - see front matter
doi:10.1016/S0022-460X(03)00134-2

1. Introduction

It has been well recognized that the presence of a crack in a structure leads to changes in the natural frequencies of the structure. When monitoring the health of the structures, the changes of this structural dynamic parameter have been used as one of the indicators to determine the incursion of crack in the structure. For beam structures, many researchers [1–8] have evaluated the effect of one or two cracks on the natural frequencies of uniform beams. Shifrin and Ruotolo [9] developed a method to deal with uniform beams with an arbitrary finite number of transverse open-cracks. Recently, Zheng and Fan [10] used a kind of modified Fourier series to determine the frequency changes of non-uniform beams with multiple cracks. In the above-mentioned methods, all are based on a kind of continuous model for a beam, in which the beam is modelled as an assembly of sub-beams connected by massless rotational springs across the cracks. A system of algebraic equations is subsequently established to determine the general eigenfrequencies.

Usually, the applications of the above methods are restricted to simple beam problems. For more complicated structures, the use of discrete method comes naturally. In the literature, many researchers have applied the finite element method (FEM) to evaluate the natural frequencies of a cracked beam, such as Gounaris and Dimarogonas [11], Qian et al. [12], and Morassi [13], just to name a few. However, the conventional FEM alone does not work well in simulating the cracked beam problems. It either needs the help of extremely refined mesh or some kinds of special element [14–19].

Recently, a so-called meshless method has emerged and has become popular. It appears to have advantages over the conventional FEM in solving boundary-value problems, in particular when costly mesh generation is required for the solutions. In the meshless method, the approximation is constructed entirely in terms of a finite number of nodes, and no element meshes need to be created. The meshless method embraces a variety of different approaches [20–25]. Their major difference lies in their ways of constructing the approximation basis function. In this paper, node-based non-uniform rational B-spline (NURBS) basis functions are used to construct the approximation function. Distribution of nodes in the NURBS representation is arbitrary and non-uniform. By adopting a kind of local symmetric weak form (LSWF)—the Petrov–Galerkin approach, the meshless method with NURBS basis functions can be formulated. The characteristic differentiability of the NURBS basis functions results in that a function with specific degrees of smoothness can be represented easily. On the other hand, the NURBS basis functions can be built over a non-uniform knot vector with some multiple knots. The magic of assigning multiple knots at selected locations leads to the deflected shape with desired degrees of discontinuity at those locations. Hence, it can yield exact solutions having interior discontinuous derivatives.

The main objective of this paper is to demonstrate the versatility of the NURBS meshless method in evaluating the natural frequencies of a beam with an arbitrary number of cracks. It enables the cracked beam to be analyzed in the usual manner as a continuous beam by inserting equivalent massless rotational springs at the crack locations to represent the local flexibility introduced by the cracks. To model the abrupt changes of slope across a crack, the approximation function is constructed by employing the quartic NURBS basis functions defined over a vector of non-uniform nodes/knots having quadruplicate knot assigned at the crack location. Detailed formulation via the local Petrov–Galerkin approach is shown in the following sections.

2. Formulation

2.1. Discretized NURBS representation with controllable degree of differentiability

The node-based NURBS basis functions are used to construct the approximation.

Given a vector, X, of non-uniformly spaced nodes/knots covering a domain Ω,

$$X = \left\{ \underbrace{x_0, \ldots, x_0}_{p+1}, x_{p+1}, \ldots, x_{m-p-1}, \underbrace{x_m, \ldots, x_m}_{p+1} \right\}, \tag{1}$$

the approximation $u^h(x)$ of dependent variable $u(x)$ over the domain Ω is defined by

$$u^h(x) = \sum_{i=0}^{n} c_i R_{i,p}(x). \tag{2}$$

In Eq. (1), p is the degree of the NURBS basis functions to be built, $m+1$ denotes the number of nodes/knots, and x_0 and x_m are co-ordinates for boundary nodes. In Eq. (2), c_i are constant coefficients to be determined, n corresponds to the number of NURBS basis functions on the interval $[x_0, x_m]$, and $R_{i,p}(x)$ is the ith NURBS basis function of degree p. The function $R_{i,p}(x)$ can be defined over the nodal vector X [26] as follows:

$$R_{i,p}(x) = \frac{N_{i,p}(x) w_i}{\sum_{j=0}^{n} N_{j,p}(x) w_j}, \tag{3}$$

where $N_{i,p}(x)$ is the ith B-spline basis function of degree p which has the recursive definition known as the Cox–deBoor algorithm as follows:

$$N_{i,0}(x) = \begin{cases} 1 & x_i \leqslant x < x_{i+1}, \\ 0 & \text{otherwise}, \end{cases}$$

$$N_{i,p}(x) = \frac{x - x_i}{x_{i+p} - x_i} N_{i,p-1}(x) + \frac{x_{i+p+1} - x}{x_{i+p+1} - x_{i+1}} N_{i+1,p-1}(x), \tag{4}$$

w_i in Eq. (3) are called weights. Specially, if w_i are equal to 1 for all i,

$$R_{i,p}(x) = N_{i,p}(x), \tag{5}$$

i.e., the B-spline basis functions are special cases of the NURBS basis functions.

It is noted from Eq. (1) that the boundary nodes/knots have multiplicity of $p+1$ if the NURBS basis functions to be built are of pth degree. As a result, the prescribed boundary conditions can be incorporated in the NURBS basis functions a priori and therefore, the essential boundary conditions can be imposed easily. In addition, the NURBS basis functions can be built over a vector of non-uniformly spaced knots, of which multiple knots can be assigned at any interior locations over the domain. The pth degree NURBS basis functions are C^{p-k} continuous at the knot with multiplicity of k. In other words, the continuity of the NURBS basis functions will decrease with increasing the knot multiplicity. Fig. 1(a) shows the quartic NURBS basis functions, $R_{i,4}(x)$, defined over the knot vector $\{0, 0, 0, 0, 0, \frac{10}{3}, \frac{10}{3}, \frac{10}{3}, \frac{10}{3}, \frac{20}{3}, 10, 10, 10, 10, 10\}$. The first derivatives of $R_{i,4}(x)$ $(i = 3, 4, 5)$ are plotted in Fig. 1(b). It is noted that a quadruplicate knot

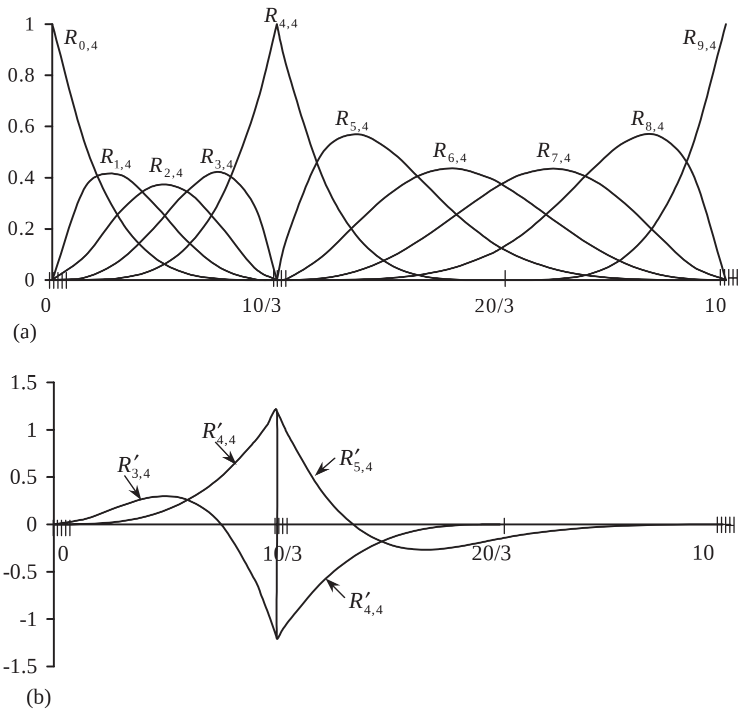

Fig. 1. Quartic NURBS basis functions and their derivatives corresponding to $X = \{0, 0, 0, 0, 0, \frac{10}{3}, \frac{10}{3}, \frac{10}{3}, \frac{10}{3}, \frac{20}{3}, 10, 10, 10, 10, 10\}$: (a) $R_{i,4}$; (b) $R'_{i,4}$.

is assigned at the location of $x = \frac{10}{3}$ and the resulting quartic NURBS basis function $R_{4,4}(x)$ and its first derivative have a cusp and a jump at the quadruplicate knot ($x = \frac{10}{3}$), respectively. Therefore, by building the NURBS basis functions over the non-uniform knot vector with multiple knots allocated at selected locations, the approximations via the NURBS basis functions will possess the desired degree of discontinuities at those locations.

2.2. NURBS meshless formulation for a multiple-cracked beam

The previous section shows that the discretized NURBS representation is an excellent candidate for solving boundary-value problems, especially for problems with discontinuities. In this section, the NURBS representation is incorporated with the meshless local Petrov–Galerkin (MLPG) approach [24] and applied to evaluate the natural frequencies of a beam with an arbitrary number of cracks.

The free vibration equation of a beam, assumed with the uniform cross-section, is

$$EI\frac{\partial^4 u(x,t)}{\partial x^4} + \rho A\frac{\partial^2 u(x,t)}{\partial t^2} = 0 \quad \text{for } 0 < x < L, \tag{6a}$$

where $u(x,t)$ is the amplitude of the transverse displacement of the beam axis, ρ is the material density, A is the cross-sectional area of the beam, EI is the bending stiffness, and L is the length of the beam. By assuming that the beam axis is under time-harmonic vibration, i.e.,

$$u(x,t) = u(x)e^{i\omega t} = ue^{i\omega t}, \tag{6b}$$

Eq. (6a) can be simplified as

$$EIu'''' = \omega^2 \rho A u \quad \text{for } 0 < x < L, \tag{6c}$$

where $u = u(x)$ is purely a function of x, and ω is the frequency of the natural transverse motion. The boundary conditions are given as

$$u(x) = u_0 \quad \text{on } \Gamma_u \qquad \text{and} \qquad \frac{\partial u(x)}{\partial x} = \theta_0 \quad \text{on } \Gamma_\theta \tag{7a}$$

$$M = M_0 \quad \text{on } \Gamma_M \qquad \text{and} \qquad V = V_0 \quad \text{on } \Gamma_V \tag{7b}$$

$$\Gamma_u \cap \Gamma_V = \emptyset \quad \text{and} \quad \Gamma_\theta \cap \Gamma_M = \emptyset, \tag{7c}$$

where M and V denote the moment and the shear force, respectively. Γ_u, Γ_θ, Γ_M, and Γ_V denote the boundary regions where displacement, slope, moment, and shear force are specified, respectively.

At the crack location, the continuity conditions on displacement, bending moment, and shear force are

$$u(x_c^-) = u(x_c^+), \tag{8a}$$

$$u''(x_c^-) = u''(x_c^+), \tag{8b}$$

$$u'''(x_c^-) = u'''(x_c^+), \tag{8c}$$

and a discontinuity condition is introduced into the rotation of the beam axis by [1]

$$u'(x_c^+) - u'(x_c^-) = \alpha u''(x_c^-), \tag{8d}$$

where x_c is the co-ordinate of the crack location and α is the flexibility of the rotational spring which is used to represent the effect of crack. For one-sided crack, α can be expressed as a function of the crack depth a and the beam depth h as follows [1,10]:

$$\alpha = 5.346 h g(\xi), \tag{9}$$

where

$$\begin{aligned} g(\xi) = {} & 1.8624\xi^2 - 3.95\xi^3 + 16.375\xi^4 - 37.226\xi^5 + 76.81\xi^6 \\ & - 126.9\xi^7 + 172\xi^8 - 143.97\xi^9 + 66.56\xi^{10}, \end{aligned} \tag{10a}$$

$$\xi = \frac{a}{h}. \tag{10b}$$

By starting from the local weighted-residual equation [24],

$$0 = \int_{\Omega_s^{(i)}} v_i (EIu'''' - \omega^2 \rho A u) \, d\Omega, \tag{11}$$

where $v_i = v_i(x)$ are weight functions and $\Omega_s^{(i)}$ is a local sub-domain located entirely inside the global domain Ω. The local weak form of Eq. (6c) can be obtained through the integration by parts of Eq. (11) as follows:

$$0 = \int_{\Omega_s^{(i)}} EIv_i'' u'' \, d\Omega - \int_{\Omega_s^{(i)}} \omega^2 \rho A v_i u \, d\Omega + [v_i EIu''']_{\partial\Omega_s^{(i)}} - [v_i' EIu'']_{\partial\Omega_s^{(i)}}, \tag{12}$$

where $\partial\Omega_s^{(i)}$ denotes the boundary of the local sub-domain $\Omega_s^{(i)}$.

The boundary of the sub-domain, $\partial\Omega_s^{(i)}$, can be decomposed into subsets of $\partial\Omega_s^{(i)} \cap \hat{\Omega}$, $\partial\Omega_s^{(i)} \cap \Gamma_u$, $\partial\Omega_s^{(i)} \cap \Gamma_\theta$, $\partial\Omega_s^{(i)} \cap \Gamma_M$, and $\partial\Omega_s^{(i)} \cap \Gamma_V$, where $\hat{\Omega}$ is the interior of the global domain. By using these decompositions, Eq. (12) can be written as follows:

$$\begin{aligned} 0 = &\int_{\Omega_s^{(i)}} EIv_i'' u'' \, d\Omega - \int_{\Omega_s^{(i)}} \omega^2 \rho A v_i u \, d\Omega + [v_i EIu''']_{\partial\Omega_s^{(i)} \cap \hat{\Omega}} - [v_i' EIu'']_{\partial\Omega_s^{(i)} \cap \hat{\Omega}} \\ &+ [v_i EIu''']_{\partial\Omega_s^{(i)} \cap \Gamma_u} - [v_i' EIu'']_{\partial\Omega_s^{(i)} \cap \Gamma_\theta} + [v_i EIu''']_{\partial\Omega_s^{(i)} \cap \Gamma_V} - [v_i' EIu'']_{\partial\Omega_s^{(i)} \cap \Gamma_M}. \end{aligned} \tag{13}$$

If the weight functions v_i are deliberately selected such that their values and derivatives vanish at $\partial\Omega_s^{(i)} \cap \hat{\Omega}$, Eq. (13) is reduced to the following equation:

$$\begin{aligned} 0 = &\int_{\Omega_s^{(i)}} EIv_i'' u'' \, d\Omega - \int_{\Omega_s^{(i)}} \omega^2 \rho A v_i u \, d\Omega + [v_i EIu''']_{\partial\Omega_s^{(i)} \cap \Gamma_u} - [v_i' EIu'']_{\partial\Omega_s^{(i)} \cap \Gamma_\theta} \\ &+ [v_i EIu''']_{\partial\Omega_s^{(i)} \cap \Gamma_V} - [v_i' EIu'']_{\partial\Omega_s^{(i)} \cap \Gamma_M}. \end{aligned} \tag{14}$$

Since the moment M and the shear force V are related to the displacement u through the equations

$$M = EIu'' \quad \text{and} \quad V = -EIu''', \tag{15}$$

the natural boundary conditions in Eq. (7b) can be written as

$$M_0 = [EIu'']_{\partial\Omega_s^{(i)} \cap \Gamma_M} \quad \text{and} \quad V_0 = -[EIu''']_{\partial\Omega_s^{(i)} \cap \Gamma_V}. \tag{16}$$

Applying Eq. (16), Eq. (14) can be expressed as

$$\begin{aligned} 0 = &\int_{\Omega_s^{(i)}} EIv_i'' u'' \, d\Omega - \int_{\Omega_s^{(i)}} \omega^2 \rho A v_i u \, d\Omega + [v_i EIu''']_{\partial\Omega_s^{(i)} \cap \Gamma_u} - [v_i' EIu'']_{\partial\Omega_s^{(i)} \cap \Gamma_\theta} \\ &- [v_i V_0]_{\partial\Omega_s^{(i)} \cap \Gamma_V} - [v_i' M_0]_{\partial\Omega_s^{(i)} \cap \Gamma_M}. \end{aligned} \tag{17}$$

When a crack occurs in the local sub-domain $\Omega_s^{(i)}$, Eq. (17) can be written as

$$\begin{aligned} 0 = &\int_{\Omega_s^{(i)}} EIv_i'' u'' \, d\Omega - \int_{\Omega_s^{(i)}} \omega^2 \rho A v_i u \, d\Omega + [v_i EIu''']_{\partial\Omega_s^{(i)} \cap \Gamma_u} - [v_i' EIu'']_{\partial\Omega_s^{(i)} \cap \Gamma_\theta} \\ &- [v_i V_0]_{\partial\Omega_s^{(i)} \cap \Gamma_V} - [v_i' M_0]_{\partial\Omega_s^{(i)} \cap \Gamma_M} \\ &+ [EIv_i(x_c^-)u'''(x_c^-) - EIv_i(x_c^+)u'''(x_c^+)] \\ &- [EIv_i'(x_c^-)u''(x_c^-) - EIv_i'(x_c^+)u''(x_c^+)]. \end{aligned} \tag{18}$$

As shown in Eq. (8), the deflection of the beam and its second and third derivatives are continuous at the crack location, but a discontinuity of the first derivative is expected there. To attain the desired degree of discontinuity, quartic NURBS basis function $R_{i,4}(x)$ over a vector of non-uniform knots having quadruplicate knot at the crack location is employed. The following conditions can be satisfied:

$$R_{i,4}(x_c^-) = R_{i,4}(x_c^+), \tag{19a}$$

$$R''_{i,4}(x_c^-) = R''_{i,4}(x_c^+), \tag{19b}$$

$$R'''_{i,4}(x_c^-) = R'''_{i,4}(x_c^+), \tag{19c}$$

$$R'_{i,4}(x_c^-) \neq R'_{i,4}(x_c^+). \tag{19d}$$

By adopting the Petrov–Galerkin method, the weight functions are chosen to be different from the approximation functions. As a special case, the same forms can be used, i.e.,

$$v_i(x) = R_{i,4}(x). \tag{20}$$

As a result, the function v_i and its first derivative v'_i can satisfy the following conditions:

$$v_i(x_c^-) = v_i(x_c^+), \tag{21a}$$

$$v'_i(x_c^-) \neq v'_i(x_c^+). \tag{21b}$$

By substituting Eqs. (8) and (21) into the local weak form equation (18), the following equation can be obtained:

$$\begin{aligned} 0 = &\int_{\Omega_s^{(i)}} EIv''_i u''\,\mathrm{d}\Omega - \int_{\Omega_s^{(i)}} \omega^2 \rho A v_i u\,\mathrm{d}\Omega + [v_i EIu''']_{\partial\Omega_s^{(i)} \cap \Gamma_u} - [v'_i EIu'']_{\partial\Omega_s^{(i)} \cap \Gamma_\theta} \\ &- [v_i V_0]_{\partial\Omega_s^{(i)} \cap \Gamma_V} - [v'_i M_0]_{\partial\Omega_s^{(i)} \cap \Gamma_M} + \frac{EI}{\alpha}[v'_i(x_c^-) - v'_i(x_c^+)][u'(x_c^-) - u'(x_c^+)]. \end{aligned} \tag{22}$$

Finally, substituting Eqs. (2) and (20) into Eq. (22) leads to a set of equations as follows:

$$(\boldsymbol{K} + \boldsymbol{K}_c - \omega^2 \boldsymbol{M}_s)\boldsymbol{c} = \boldsymbol{f}, \tag{23}$$

where $\boldsymbol{K}$ denotes the stiffness matrix of the beam without a crack. $\boldsymbol{K}_c$ is a correction matrix for $\boldsymbol{K}$ due to the crack. $\boldsymbol{M}_s$ and $\boldsymbol{f}$ denote the mass matrix and external load vector, respectively. The entries in $\boldsymbol{K}$, $\boldsymbol{K}_c$, $\boldsymbol{M}_s$, and $\boldsymbol{f}$ are defined by

$$K_{ij} = \int_{\Omega_s^{(i)}} EIR''_{i,4}R''_{j,4}\,\mathrm{d}\Omega + EI[R_{i,4}R'''_{j,4}]_{\partial\Omega_s^{(i)} \cap \Gamma_u} - EI[R'_{i,4}R''_{j,4}]_{\partial\Omega_s^{(i)} \cap \Gamma_\theta}, \tag{24a}$$

$$K_{c,ij} = \frac{EI}{\alpha}[R'_{i,4}(x_c^-) - R'_{i,4}(x_c^+)][R'_{j,4}(x_c^-) - R'_{j,4}(x_c^+)], \tag{24b}$$

$$M_{s,ij} = \int_{\Omega_s^{(i)}} \rho A R_{i,4} R_{j,4}\,\mathrm{d}\Omega, \tag{24c}$$

$$f_i = [R_{i,4}V_0]_{\partial\Omega_s^{(i)} \cap \Gamma_V} + [R'_{i,4}M_0]_{\partial\Omega_s^{(i)} \cap \Gamma_M}. \tag{24d}$$

For an arbitrary number of cracks, Eq. (24b) can be rewritten as

$$K_{c,ij} = \sum_{n_c} \frac{EI}{\alpha_{n_c}}[R'_{i,4}(x_{c,n_c}^-) - R'_{i,4}(x_{c,n_c}^+)][R'_{j,4}(x_{c,n_c}^-) - R'_{j,4}(x_{c,n_c}^+)], \tag{24e}$$

where n_c represents the number of cracks.

It is worth noting that the matrix $\boldsymbol{K}_c$ represents the cracks' softening effect on the stiffness of the beam. By adding it into the matrix $\boldsymbol{K}$, a general stiffness matrix for the cracked beam, $\bar{\boldsymbol{K}}$, can be obtained as

$$\bar{\boldsymbol{K}} = \boldsymbol{K} + \boldsymbol{K}_c. \tag{25}$$

Substituting Eq. (25) into Eq. (23), the natural frequencies of the cracked beam, ω, can be evaluated by solving the following equation of motion:

$$(\bar{\boldsymbol{K}} - \omega^2 \boldsymbol{M}_s)\boldsymbol{c} = \boldsymbol{f}. \tag{26}$$

3. Numerical examples

To validate the present method, the natural frequencies of cracked beam with different crack depths and locations are evaluated. Numerical results are compared with available published results.

3.1. Example 1

Firstly, a simply supported beam with a single crack is considered. The crack has variable position from the left end to the right end of the beam and its depth also varies ($a = 10$, 15, 20, or 25 mm). The changes of first three natural frequencies, $\Delta\omega$, are calculated by the present method. Results are compared with those obtained by the conventional FE method [6]. As shown in Figs. 2–4, the results from the present method coincide well with the FEM results in Ref. [6]. It is worth noting that the finite element solutions needs a well-defined finite element mesh in the region adjacent to the crack as shown in Fig. 5 [6] whereas no element mesh needs to be constructed in the present method. For easy visualization and highlighting the advantages of the present method, the vibration mode shapes of the beam are plotted. Fig. 6(a) shows the first deflection mode shape for the beam with the single crack at mid-span. The corresponding slope is

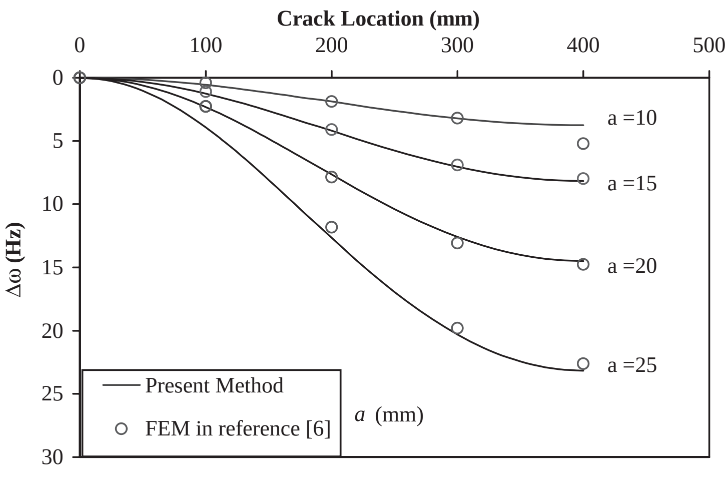

Fig. 2. Effect of single crack on the first natural frequency of a simply supported beam.

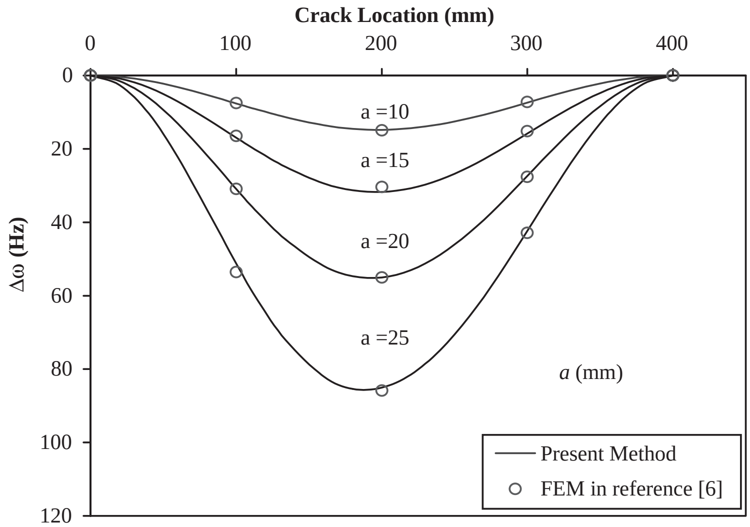

Fig. 3. Effect of single crack on the second natural frequency of a simply supported beam.

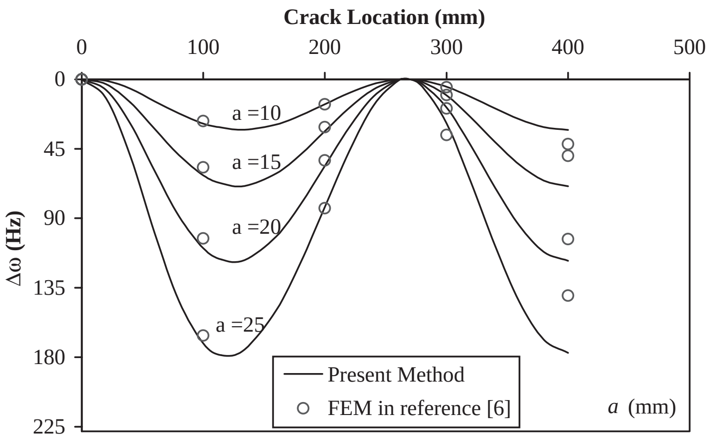

Fig. 4. Effect of single crack on the third natural frequency of a simply supported beam.

plotted in Fig. 6(b). As expected, a discontinuity in slope is represented exactly at the crack location. It cannot be obtained by the conventional FEM. In addition, the solutions for multiple open-cracks of various depths at various locations can be obtained easily by the present formulation. No cumbersome remeshing is needed.

3.2. Example 2

Subsequently, a cantilever beam with two cracks is analyzed by the present method. For the purpose of comparing the results with those in Ref. [9] the same properties of the beam are used as follows: length $L = 800$ mm, rectangular cross-section with width $b = 20$ mm and height $h =$

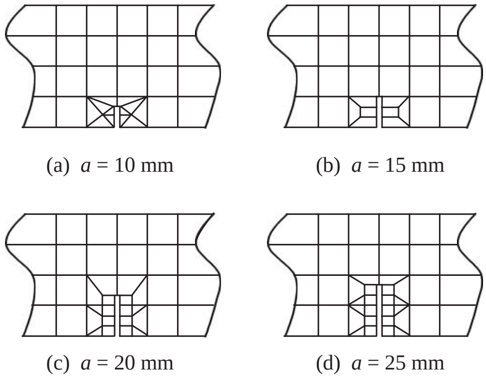

Fig. 5. Finite element discretization around crack in beam [6], a is the crack depth: (a) $a = 10$ mm; (b) $a = 15$ mm; (c) $a = 20$ mm; (d) $a = 25$ mm.

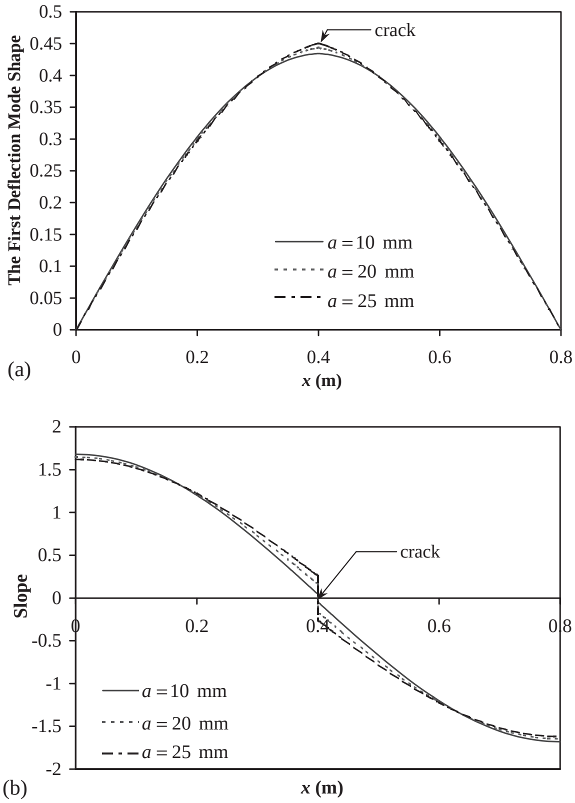

Fig. 6. Vibration mode shape for the first natural frequency: (a) deflection, (b) slope.

20 mm, Young's modulus $E = 2.1 \times 10^{11}$ N/m^2, and material density $\rho = 7800$ kg/m^3. The first crack has a fixed location at $x_{c1} = 120$ mm and a depth of $a_1 = 2$ mm. The second crack's position varies from the clamped end to the free end of the beam and three depths are tested ($a_2 = 2$, 4, and 6 mm). Figs. 7–9 show the ratios of ω_i/ω_{0i} versus the location of the second crack x_{c2}, where ω_i

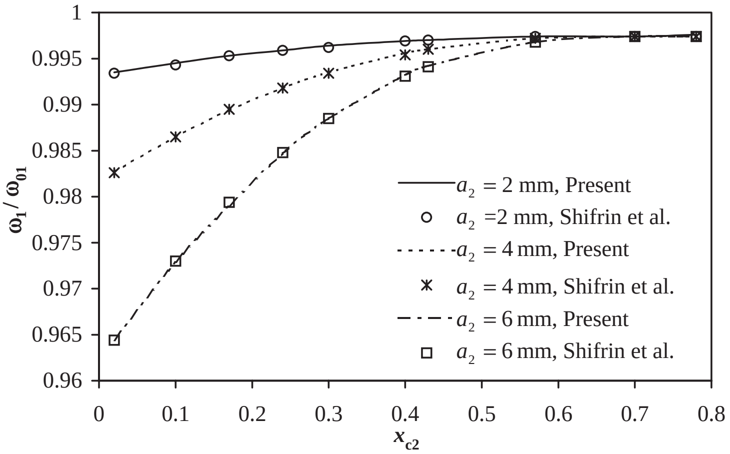

Fig. 7. Effect of the second crack on the first natural frequency of a cantilever beam.

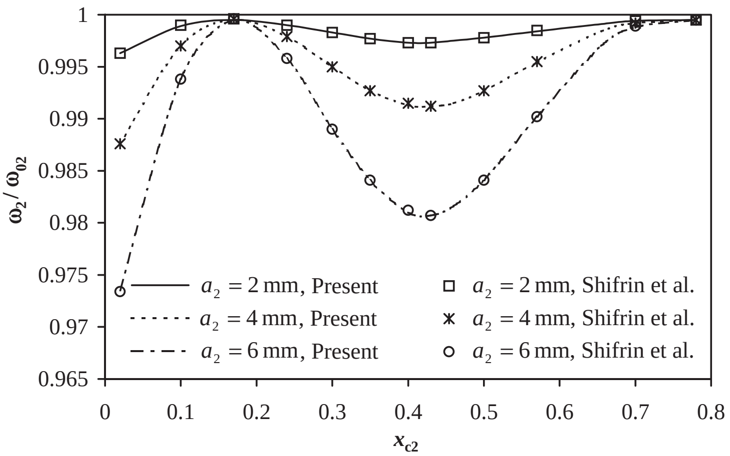

Fig. 8. Effect of the second crack on the second natural frequency of a cantilever beam.

and ω_{0i} are the first three natural frequencies of the cracked and uncracked beam, respectively. It can be observed that the results obtained by the present method agree very well with those published in Ref. [9].

4. Conclusions

The formulation of the NURBS meshless method is shown in this paper. The method is applied to examine the crack-induced eigenfrequency changes of beam structure. The beam can have any boundary conditions, and have arbitrary number of cracks. To impose the discontinuous conditions for the rotation of the beam at the crack locations, a non-uniform knot vector having quadruplicate knots at the crack locations is used to build the quartic NURBS basis functions.

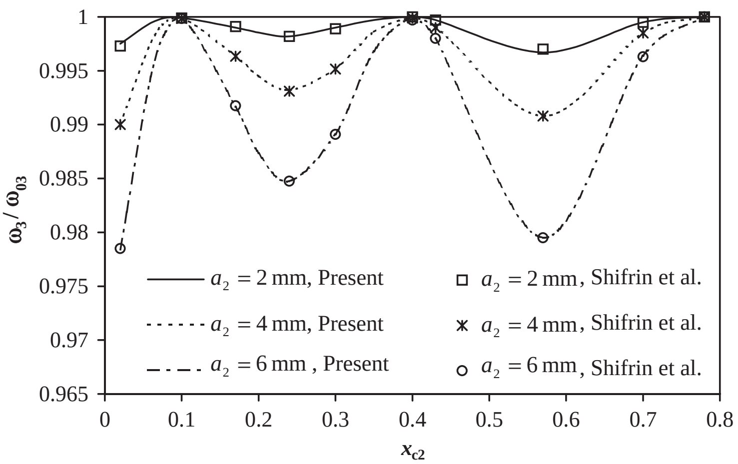

Fig. 9. Effect of the second crack on the third natural frequency of a cantilever beam.

Subsequently, adopting the local Petrov–Galerkin method leads to a generalized stiffness matrix for the cracked beam. The natural frequencies of the cracked beam can then be evaluated by solving an equation of motion. The great advantage of the present method is derived from the discretized NURBS basis functions, which allow easy modelling of different orders of discontinuities. Numerical examples show that the present method is effective and easy to use.

References

[1] P.F. Rizos, N. Aspragatos, A.D. Dimarogonas, Identification of crack location and magnitude in a cantilever beam from the vibration modes, Journal of Sound and Vibration 138 (1990) 381–388.
[2] W.M. Ostachowicz, M. Krawczuk, Analysis of the effect of cracks on the natural frequencies of a cantilever beam, Journal of Sound and Vibration 150 (1991) 191–201.
[3] R. Ruotolo, C. Surace, C. Mares, Theoretical and experimental study of the dynamic behaviour of a double-cracked beam, Proceedings of the 14th International Modal Analysis Conference, 1996, pp. 1560–1564.
[4] T.G. Chondros, A.D. Dimarogonas, Identification of cracks in welded joints of complex structures, Journal of Sound and Vibration 69 (1980) 531–538.
[5] R.Y. Liang, F. Choy, J. Hu, Detection of cracks in beam structures using measurements of natural frequencies, Journal of the Franklin Institute 328 (1991) 505–518.
[6] R.Y. Liang, J. Hu, F. Choy, Theoretical study of crack-induced eigenfrequency changes on beam structures, Journal of Engineering Mechanics 118 (1992) 384–396.
[7] R.Y. Liang, J. Hu, F. Choy, Quantitative NDE techniques for assessing damages in beam structures, Journal of Engineering Mechanics 118 (1992) 1468–1487.
[8] J. Hu, R.Y. Liang, An integrated approach to detection of cracks using vibration characteristics, Journal of the Franklin Institute 330 (1993) 841–853.
[9] E.I. Shifrin, R. Ruotolo, Natural frequencies of a beam with an arbitrary number of cracks, Journal of Sound and Vibration 222 (1999) 409–423.
[10] D.Y. Zheng, S.C. Fan, Natural frequency changes of a non-uniform beam with multiple cracks via modified Fourier series, Journal of Sound and Vibration 242 (2001) 701–717.
[11] G. Gounaris, A.D. Dimarogonas, A finite element of a cracked prismatic beam for structural analysis, Computers and Structures 28 (1988) 309–313.

[12] G.L. Qian, S.N. Gu, J.S. Jiang, The dynamic behaviour and crack detection of a beam with a crack, Journal of Sound and Vibration 138 (1990) 233–243.

[13] A. Morassi, Crack-induced changes in eigenfrequencies of beam structures, Journal of Engineering Mechanics 119 (1993) 1768–1803.

[14] O.C. Zienkiewicz, J.Z. Zhu, N.G. Gong, Effective and practical h-p-version adaptive analysis procedures for the finite element method, International Journal for Numerical Methods in Engineering 28 (1989) 879–891.

[15] Z. Yosibash, B. Szabo, Numerical analysis of singularities in two-dimension—part 1: computation of eigenpairs, International Journal for Numerical Methods in Engineering 38 (1995) 2055–2082.

[16] H.S. Oh, I. Babuska, The method of auxiliary mapping for the finite element solutions of elasticity problems containing singularities, Journal of Computational Physics 121 (1995) 193–212.

[17] Z. Yosibash, B. Schiff, A super-element for the finite element solution of two-dimensional elliptic problems with boundary singularities, Finite Element Analysis and Design 26 (1997) 315–335.

[18] T. Belytschko, T. Black, Elastic crack growth in finite elements with minimal remeshing, International Journal for Numerical Methods in Engineering 45 (5) (1999) 601–620.

[19] I. Babuska, B. Anderson, B. Guo, Finite element method for solving problems with singular solutions, Journal of Comput. and Applied Mathematics 74 (1–2) (1996) 51–70.

[20] W.K. Liu, S. Jun, Y.F. Zhang, Reproducing kernel particle methods, International Journal for Numerical Methods in Fluids 20 (1995) 1081–1106.

[21] B. Nayroles, G. Touzot, P. Villon, Generalizing the finite element method: diffuse approximation and diffuse elements, Computational Mechanics 10 (1992) 307–318.

[22] T. Belytschko, Y.Y. Lu, L. Gu, Element-free Galerkin methods, International Journal for Numerical Methods in Engineering 37 (1994) 229–256.

[23] C.A. Duarte, J.T. Oden, *Hp* Clouds—an *hp* meshless method, Numerical Methods for Partial Differential Equations 12 (1996) 673–705.

[24] S.N. Atluri, T. Zhu, A new meshless local Petrov–Galerkin (MLPG) approach in computational mechanics, Computational Mechanics 22 (1998) 117–127.

[25] Y. Krongauz, T. Belytschko, EFG approximation with discontinuous derivatives, International Journal for Numerical Methods in Engineering 41 (1998) 1215–1233.

[26] L.A. Piegl, W. Tiller, The NURBS Book, Springer, New York, 1997.